Plant Soil
https://doi.org/10.1007/s11104-025-07412-8

RESEARCH ARTICLE

Speciation of cadmium and copper in the herbaceous flowering hyperaccumulator *Bidens pilosa* L. and their detoxification mechanisms

Siqi Wang · Jiayi Bai · Huiping Dai · Jie Zhan · Liping Ren · Brett H. Robinson · Chengzhi Jiang · Shuang Cui · Lidia Skuza · Shuhe Wei

Received: 30 November 2024 / Accepted: 24 March 2025

Abstract

Purpose We aimed to elucidate the speciation of Cd and Cu in the herbaceous flowering hyperaccumulator *Bidens pilosa* L. and their detoxification mechanisms.

Methods Seedlings of *B. pilosa* were grown in hydroponic solution in a greenhouse. FTIR was used to determine differences in functional groups (including -OH, $-CH_2$, $-CH(CH_3)_2$, $-CO_2H$ and $-NH_2$) in molecular compounds from different tissue cells under different concentrations of Cd and Cu treatments. The subcellular distributions and chemical forms of Cd and Cu were determined by using differential centrifugation and sequential extraction methods.

Results FTIR revealed that the abundance of -OH, $-CH_2$ groups, acid amides and lipids increased with increasing Cd concentrations. indicating that corresponding macromolecules, such as alcohols and phenols, proteins and lipids in cells in the stems/roots of *B. pilosa* reduced Cd stress. The results showed that $-CH(CH_3)_2$ groups bound Cd on the surface of the root cells. In contrast, the amount of $-CH(CH_3)_2$ groups was reduced with increasing Cu stress. The amount of $-CH(CH_3)_2$ groups and protein with acid

Responsible Editor: Juan Barcelo.

S. Wang (✉) · C. Jiang · S. Cui
Academy of Environmental and Chemical Engineering, Shenyang Ligong University, Shenyang 110159, Liaoning, China
e-mail: wang3331336637@126.com

S. Wang · J. Bai · L. Ren · S. Wei (✉)
Key Laboratory of Pollution Ecology and Environment Engineering, Institute of Applied Ecology, Chinese Academy of Sciences, Shenyang 110016, China
e-mail: shuhewei@iae.ac.cn

H. Dai (✉)
College of Biological Science & Engineering, Shaanxi Province Key Laboratory of Bio-Resources, Qinling-Bashan Mountains Bioresources Comprehensive Development C.I.C, State Key Laboratory of Biological Resources and Ecological Environment Jointly Built by Qinba Province and Ministry, Shaanxi University of Technology, Hanzhong 723001, China
e-mail: daihp72@snut.edu.cn

J. Zhan
Liaoning Vocational College of Medicine, Shenyang 110101, China

B. H. Robinson
School of Physical and Chemical Sciences, University of Canterbury, Christchurch 8041, New Zealand

L. Skuza
Institute of Biology, Centre for Molecular Biology and Biotechnology, University of Szczecin, 71-415 Szczecin, Poland

Published online: 03 April 2025

amides increased in cells in the stems of *B. pilosa* under Cd treatments. Subcellular distributions and chemical speciation analyses revealed that Cd was mainly sequestered in cytoplasm and cell walls of *B. pilosa* roots. In contrast, Cu was mostly bound in the cell walls. In the roots, the most Cd and Cu were ethanol extractable, indicating relative lability with a high potential to be translocated to the shoots. In the stems and leaves most Cd was bound in the cell walls. But there were no significant changes for the proportion of ethanol-extracted Cu in stems and leaves.

Conclusions *B. pilosa* is a Cd hyperaccumulator, but not a Cu hyperaccumulator. The key compounds associated with Cd hyperaccumulation in *B. pilosa* were alcohols, phenols, acid amides and lipids.

Keywords *Bidens pilosa* L. · Cadmium · Copper · Functional groups · Subcellular distribution · Chemical form

Introduction

Hyperaccumulators and accumulators are plants, with heavy metal concentrations in the shoots that are several times higher than non-accumulator plants, without a significant reduction in biomass (Xu et al. 2022). Hyperaccumulator plants have mechanisms for both the translocation and tolerance of heavy metals. Plants that hyperaccumulate Cd and Cu are hypothesised to detoxify these elements through immobilisation on cell walls, chelation with organic acids from root exudates, sequestration in the the vacuole, the production of antioxidant enzymes, and increased synthesis of proteins, amino acids and polysaccharides (Heredia et al. 2022; Pasricha et al. 2021). Elucidating the mode and route of transport, and the mechanisms of Cd or Cu enrichment in accumulator and hyperaccumulator plants can inform the the management of contaminated sites (Feng et al. 2019; Yang et al. 2017). Yet there is a lacuna of information on the role of functional groups in accumulator and hyperaccumulator plants.

Black-jack (*Bidens pilosa* L.) is an annual species of herbaceous flowering plant in the asteraceae family. It is native to the tropical regions of America and widely distributed in tropical and subtropical regions of Asia. *B. pilosa* propagates by seeds that are transported by wind, water, and through mechanical adhesion to animals (Cai et al. 2022; Omara et al. 2020; Tolmacheva et al. 2014). Wei and Zhou (2008) reported that *B. pilosa* exhibited the characteristics of Cd hyperaccumulator accumulating and tolerating Cd concentrations manifold higher than other species growing in the same environment. Cd concentrations in *B. pilosa* leaves and stems were up to 192 mg/kg and 115 mg/kg, respectively, with soil Cd concentrations of 100 mg/kg. The authors also showed that *B. pilosa* was not an accumulator or hyperaccumulator of Cu, as shoot biomass decreased significantly compared to controls in soil containing 400 mg/kg Cu, while root and shoot Cu concentrations were 39 mg/kg and 12 mg/kg, respectively. Wei et al. (2018) showed that the root biomass and net photosynthetic rate increased significantly when *B. pilosa* was treated with 60 mg kg^{-1} Cd for five months, and Cd concentration in the shoots was up to 295 mg kg^{-1}. Yu et al. (2022a) assessed the Cd uptake *B. pilosa* and five other plant species in a field study and found that the translocation factor (TF) of *B. pilosa* was significantly higher than those of the other plant species except *Solanum nigrum* L, reaching 2.46 ± 0.02. Sun et al. (2009) demonstrated that the growth of *B. pilosa* plants was promoted by soil Cd concentrations up to mg kg^{-1}, with an increase in shoot biomass by 13.8% compared to the controls. The Cd concentrations of stems and leaves were 108 and 144 mg kg^{-1}, respectively, at Cd soil concentration of 8 mg kg^{-1}.

Potentially, fourier transform infrared spectroscopy (FTIR) may be used to identify the composition of critical organic compounds that responsible Cd and Cu tolerance and accumulation (Yu et al. 2018, 2020; He et al. 2020). Using FTIR, Sharma and Uttam (2017) showed that the pectin content in the cell wall of wheat seedlings increased significantly under 500, 600, 700, and 800 mg L^{-1} nano-CuO stress, and the characteristic peaks at 1240 and 1320 cm^{-1} were altered with increasing nano-CuO concentrations. An increasing lignin content was determined in leaves on the basis of an increased band intensity at the area of 1507 cm^{-1}. Reduced band areas of $-CH_2$ lipid groups indicated that treatments with nano-CuO increased lipid peroxidation in plants. Liu et al. (2021) studied cell wall polysaccharides from beet (*Beta vulgaris* L.), kiwifruit (*Actinidia chinensis* Planch.), apple (*Malus pumila* Mill.) and found that the absorbance peaks at 1035 cm^{-1} were due to xylose-containing hemicelluloses, those at 1065 and 807 cm^{-1} were attributed

to mannose-containing hemicelluloses, while the characteristic peaks at 1740 and 1600 cm^{-1} correspond to homogalacturonans based on the degree of methylation. Suresh et al. (2016) studied the effects of nano-CuO stress on biochemical constituents of peanut (*Arachis hypogaea* L.) leaves and found characteristic peaks at 1033, 1636 and 2923 cm^{-1}, which corresponded to carbohydrates, proteins and lipids in leaf tissues, respectively. Sharma and Uttam (2019) studied the biochemical response of wheat (*Triticum aestivum* L.) seedling leaves to nano-Al_2O_3 stress and observed that the intensities of characteristic peaks corresponding to pectin, cellulose, lignin and hemicellulose were significantly more intense as a result of 3 mM nano-Al_2O_3 treatments, and the peak areas related to methylene and amine groups visibly increased with raising nano-Al_2O_3 concentrations, which indicated that the defense strategy of wheat seedlings against nano-Al_2O_3 toxicity was based on improving lipids, amino acids and proteins in leaves. Yu et al. (2020) characterised the physiological responses of *Conyza canadensis* (L.) Cronq. to 1 ~ 7 mg L^{-1} of Cd stress using FTIR and found three characteristic peaks (3417 ~ 3429 cm^{-1}, 1380 ~ 1386 cm^{-1}, and 1631 ~ 1637 cm^{-1}), which corresponded to hydroxy, carboxyl and acid amide groups. These functional groups are all involved in Cd binding and adsorption. Chow and Ting (2019) found that changes in the plant cell wall chemical composition could be inferred using FTIR and the intensity ratios of absorption peaks (I_{1458}/I_{1158} and I_{1458}/I_{1375}), which corresponded to the synthesis and decomposition of lignin and carbohydrates. Yu et al. (2021) demonstrated that the removal of pectins markedly reduced the peak areas at 3477 cm^{-1}, 3414 and 1619 cm^{-1} in the cell wall of rice (*Oryza sativa* L.) roots, which corresponded to the lower amount of carboxyl, hydroxyl, and nitrogen–hydrogen bonds of amines, and carbonyl amide I functional groups. The latter results suggested that the removal of hemicellulose and pectin decreased the relative peak areas at 1251, 1430, 1515, 1730 and 2920 cm^{-1}. These authors also investigated the mechanisms of Cd binding to polysaccharides in the root cell wall of Cd-excluding rice cultivars using FTIR and suggested that the carboxyl and hydroxyl groups in pectin and hemicellulose were beneficial for Cd immobilization and retention.

Zou et al. (2023) reported that Ca addition could alleviate physiological toxicity of Chinese willow trees (*Salix matsudana* Koidz) under Cd stress, decrease Cd uptake by roots, increase transport from root to shoot, elevate the proportion of Cd in the cytoplasm and reduce Cd deposition in cell wall, and lead to Cd subcellular redistribution. The chemical form of Cd was changed from HCl-extracted to NaCl-extracted. Li et al (2023) investigated the subcellular mechanism of Cd accumulation by black nightshade (*S. nigrum* L.), and found that vacuolar compartmentalisation was a dynamic regulatory process with continuous glutathione consumption, and the role of glutathione in vacuoles was to chelate and store Cd. Wu et al. (2016) investigated the principles of Cd accumulation, localization, subcellular distribution and chemical forms in *Salix matsudana* Koid roots, and found that Cd concentration in the different subcellular fractions was in the following order: cell wall > cytoplasm > organelle, after treatment with 100 μM Cd for 24 h. Meanwhile, the proportion of Cd chemical forms in roots was ordered as follows: NaCl-extracted > CH_3COOH-extracted > HCl-extracted > water-extracted > ethanol-extracted > residue-extracted. Teng et al. (2021) studied the detoxification mechanism and vacuolar compartmentalizationin in the leaf of *S. nigrum*, and discovered that the majority of dissolved Cd ions or combined Cd was trapped inside or outside of the vacuoles. More than 99% Cd was stored in vacuoles after treatment with 25 μM Cd. Furthermore, and 3 ~ 10 times of Cd accumulation was combined inside the vacuole than that of outside.

Some studies have focused on Cd accumulation by *B. pilosa.* However, there are no reports on the differences between Cu and Cd detoxification by *B. pilosa.* Therefore, the aims of this study were: (1) to determine the differences between Cd hyperaccumulation by *B. pilosa* compared with Cu; (2) to identify compounds and functional groups of *B. pilosa* associated with elevated Cd in relation to Cu by FTIR, with special attention to differences in the functional group characteristics; (3) to understand the mechanism behind Cd and Cu resistance in *B. pilosa* by investigating the subcellular distribution and chemical forms. It was hypothesized that the functional groups characteristics, subcellular distributions and chemical forms would show significant differences in the

mechanisms of *B. pilosa* Cd hyperaccumulation and detoxification compared to Cu.

Materials and methods

Plant culture and treatment

A series of experiments was carried out in a greenhouse located in the Shenyang Institute of Applied Ecology of the Chinese Academy of Sciences (123°59′E and 41°92′N). *B. pilosa* seeds were collected from the surrounding park, which has uncontaminated soil, when they reached the maturity phase. On July 4th, 2024, twenty seeds of *B. pilosa* were sown after surface disinfection in nursery pots (20 cm × 30 cm × 5 cm) filled with sterile sand (quartz sand, AR, 14808–60-7, particle size was 0.3 mm ~ 0.6 mm, National Pharmaceutical Group Corporation, Shanghai, China) to a depth of 2 cm. Seeds were cultivated in a greenhouse with a constant temperature (24 ± 2℃) at an 8/16 h dark/light photoperiod. Half strength Hoagland solution (100 mL) was added every two days. When the height of most seedlings reached 5 cm, uniform seedlings were transplanted (11 per container) to transparent plastic containers (25 cm × 10 cm × 16 cm) to observe root growth; containers were filled with sterile 1/2-strength Hoagland solution with Cd or Cu under 24 h aeration with an ACO-9610 adjustable silent oxygen pump (Hailea, Guangdong, China), and 0.025 mM KH_2PO_4 was replaced with KCl to avoid the formation of Cd or Cu phosphate precipitates in the solution. The roots of *B. pilosa* seedlings were stressed with 0.5, 2, 8, 16 mg L^{-1} Cd (as $CdCl_2 \cdot 2.5\ H_2O$) and Cu (as $CuSO_4 \cdot 5\ H_2O$) treatments. The pH of the solutions was maintained at 5.5 ± 0.2 by adding 2 mM MES (2-morpholinoethanesulphonic acid). Sterile nutrient solutions without Cd or Cu were used as controls, and the solutions from each container were replaced every three days. Each treatment was repeated thrice and containers were arranged in a randomized block design in the experiments. Twenty-five containers were rotated every 12 h to maintain uniform environmental conditions. The plants were harvested seven days after transplanting. Meanwhile, every repetition of treatments was analyzed three times from July 15th to August 15th, 2024.

FTIR spectra and determination of biomass and Cd/Cu concentration

Briefly, roots, stems and leaves of *B. pilosa* seedlings were separated, freeze-dried, pulverized with KBr (v/v = 1:100) and sieved through a 200-μm mesh, FTIR spectral data (4000 to 400 cm^{-1}) of individual tissue parts were obtained using a FTIR spectrometer (Nicolet 6700, Thermo Fisher Scientific, Massachusetts, USA).

The collected roots and shoots of *B. pilosa* were separated and washed with ultrapure water. The samples were oven-dried at 100℃ for 30 min, and then at 80℃ to a constant weight. The biomass was measured using a balance to the nearest 0.001 g The samples of roots, stems and leaves subjected to various treatments were digested according to a method described by Zeng et al. (2019), with modifications; Cd and Cu concentrations were determined using ICP-OES (iCAP™ 7200, Thermo Fisher Scientific, Massachusetts, USA) (Hamid et al. 2019). The measured Cd concentration in *B. pilosa* seedlings was checked based on the standard reference material for plant composition analysis (GBW07604, GSV-3, poplar leaves) (Wei et al. 2010). The blanks and samples were determined in triplicate. The limits of detection (LOD) and quantification (LOQ) were 0.0018 and 0.0037 mg/kg, respectively. The measured values of Cd and Cu in certified materials were 0.29 ± 0.01 and 9.3 ± 1.0 mg/kg, and the values of relative standard deviation (RSD) and Cd recovery rate were 3% and 90 ± 1%, respectively.

The translocation factor (TF) was determined on the basis of the ratio of the Cd shoot to root Cd concentration according to the following formula (2.1):

$$TF = \frac{Cd_{shoot}}{Cd_{root}} \tag{2.1}$$

Analysis of subcellular distribution of Cd and Cu

The subcellular tissues of roots, stems and leaves from *B. pilosa* seedlings were separated by differential centrifugation methods (Pan et al. 2019; Luo et al. 2024). Firstly, 0.5 g fresh samples were frozen with liquid nitrogen, and ground with a chilled mortar and pestle, and then homogenized with 5 mL of 50 mM Tris–HCl (pH = 7.5) and 1 mM $C_4HO_2S_2$ (DTT) as extraction buffers. Secondly, after the samples were centrifuged

at 600 × *g* for 10 min, the cell wall (FI) was obtained from the precipitate. The supernatants were further centrifuged at 2000 × *g* for 10 min, and the resulting precipitate representing the plastid (chloroplasts in leaves) (FII). Thirdly, the remaining supernatants were further centrifuged at 10,000 × *g* for 20 min, and the resulting precipitates and supernatants representing the mitochondria (FIII) and cytoplasm (FIV), respectively. The above centrifugation procedures were all completed using high speed centrifuge (Microfuge 20/20R, Beckman Coulter, Brea, California, USA) at 4 ℃. Meanwhile, the Cd/Cu concentrations in three fractions were determined according to the method used to analyze plant Cd/Cu concentrations.

Extraction of Cd and Cu in different chemical forms

Different Cd and Cu chemical forms of roots, stems and leaves from *B. pilosa* seedlings were extracted by sequential extraction method (Pan et al. 2019; An et al. 2023). 0.5 g fresh samples were frozen and ground, and then homogenized with different extraction solutions (20 mL) as follows: (1) 80% ethanol; (2) deionized water; (3) 1 M NaCl; (4) 2% CH_3COOH; (5) 0.6 M HCl; (6) Residues. Firstly, the different homogenates were shaken for 24 h at 24 ℃ and centrifuged at 5000 rpm for 10 min, the first supernatant was collected in a conical beaker. Meanwhile, 10 mL corresponding extraction solution was added into the precipitate was shaken for 2 h at 24 ℃. Secondly, the homogenate was centrifuged at 5000 rpm for 10 min, the second supernatant was mixed with the first one as tested solution, and the second precipitates were taken as residues. Finally, different chemical forms of Cd and Cu were obtained by the above procedures. The Cd/Cu concentrations in second precipitates were determined according to the method used to analyze plant Cd/Cu concentrations.

Data processing and statistical analysis

Microsoft Excel 2022 and SPSS (26.0) software was used to calculate the means and standard deviations of the data ($n = 3$). LSD was used to test the inconsistencies in FTIR results (e.g., peak intensity, peak shift) under different Cd and Cu treatments, and the significant differences ($p < 0.05$) for individual treatment were assessed by using DPS (V9.50) (Pan et al. 2016; Wang et al. 2022). The determination and quantitative analysis of characteristic peaks in FTIR spectra of *B. pilosa* was conducted using Origin (V10.50).

Results

B. pilosa hyperaccumulation characteristics for Cd

Table 1 shows that the biomass of *B. pilosa* roots and shoots did not change significantly under Cd stress in the concentration range of 0.5 to 2 mg L^{-1}, suggesting that the roots were highly tolerant within this Cd concentration range. The dry weight of shoots and roots under 16 mg L^{-1} Cd stress was reduced by 31% and 49% respectively, compared to controls. Root and shoot biomass decreased with increasing Cu levels

Table 1 Biomass and Cd and Cu concentration of *Bidens pilosa* L

Treatment	Biomass (g pot^{-1})		Concentration (mg kg^{-1})		TF
	Root	Shoot	Root	Shoot	
Control	0.94 ± 0.07a	0.84 ± 0.04a	2.92 ± 0.78e	3.56 ± 0.18e	1.28 ± 0.36
Cd 0.5	0.90 ± 0.07a	0.81 ± 0.03a	78.82 ± 4.09d	99.64 ± 5.42d	1.26 ± 0.02
Cd 2	0.91 ± 0.08a	0.79 ± 0.01a	483.42 ± 7.16c	848.47 ± 169.66c	1.76 ± 0.37
Cd 8	0.71 ± 0.04b	0.55 ± 0.03b	4797.66 ± 54.96b	5100.69 ± 284.48b	1.06 ± 0.05
Cd 16	0.65 ± 0.04c	0.43 ± 0.03c	6236.95 ± 71.44a	7764.55 ± 441.39a	1.24 ± 0.06
Control	0.94 ± 0.07a	0.84 ± 0.04a	12.31 ± 1.16c	11.86 ± 1.16b	0.97 ± 0.09
Cu 0.5	0.76 ± 0.08b	0.65 ± 0.07b	55.60 ± 22.73c	18.28 ± 0.95b	0.37 ± 0.17
Cu 2	0.36 ± 0.02c	0.54 ± 0.08bc	1477.65 ± 88.05c	28.75 ± 1.86b	0.02 ± 0.01
Cu 8	0.29 ± 0.02c	0.49 ± 0.07 cd	9478.60 ± 1484.25b	154.47 ± 44.01a	0.02 ± 0.01
Cu 16	0.17 ± 0.02d	0.41 ± 0.06d	12,322.18 ± 1929.53a	213.66 ± 60.90a	0.02 ± 0.01

Means of columns in different Cd or Cu treatments and controls marked with the same lowercase letters were not significantly different at $p < 0.05$

(from 0.5 to 16 mg L^{-1}), and root and shoot biomass was reduced by 82% and 51% in 16 mg L^{-1} Cu treatments compared to controls.

Cd accumulation in *B. pilosa* roots and shoots increased with increasing Cd concentrations relative to controls (Table 1). Cd concentrations in shoots were significantly higher than in roots after individual Cd treatments. The TF of *B. pilosa* was always > 1 for all Cd treatments, indicating its compliance with basic characteristics of a Cd hyperaccumulator. The highest TF was recorded in the treatments with 2 mg L^{-1} Cd. Cu accumulation in *B. pilosa* roots and shoots raised with increasing Cu concentrations in comparison to controls. Cu concentrations in shoots were significantly lower than in roots in individual Cu treatments. The TF was always < 1 in all Cu treatments, indicating that this plant was not a Cu hyperaccumulator.

FTIR differences between *B. pilosa* accumulating Cd and Cu

Functional groups in individual parts of *B. pilosa* under different Cd concentrations are shown in Fig. 1A, B, C. We selected five relatively significant characteristic peaks (3394 ± 20 cm^{-1}, 2925 ± 1 cm^{-1}, 1646 ± 2 cm^{-1}, 1390 ± 9 cm^{-1} and 1063 ± 12 cm^{-1}) from the range between 4000 and 400 cm^{-1}, which corresponded to the following functional groups and biochemical regions: alcohols and phenols, composed of -OH (3700 ~ 3200 cm^{-1}) and -CH_2 groups (anti-symmetric C-H stretching vibration bands at 2930 cm^{-1}), protein with acid amides (1700 ~ 1600 cm^{-1}), -$CH(CH_3)_2$ groups (symmetric C-H stretching vibration bands at 1380 cm^{-1}), and lipids, consisting of fatty acid long chains (C-O stretching vibration bands at 1300 ~ 1000 cm^{-1}) (Yu et al. 2018, 2020, 2022b). As shown in Fig. 2A, the peaks at 3410, 2924, 1646 and 1056 cm^{-1} in the root spectrum reached their maximum in 8 mg L^{-1} Cd treatment, the abundance of -OH, -CH_2 groups, acid amides and lipids increased with increasing Cd concentrations, indicating their involvement in the root cell co-precipitation and complexation in response to Cd toxicity. There was also a significant increase in 1385 cm^{-1} peaks at a Cd concentration of 2 mg L^{-1}, indicating that the amount of -$CH(CH_3)_2$ groups was relatively higher compared to controls and other Cd treatments. The absorbance intensities of peaks at

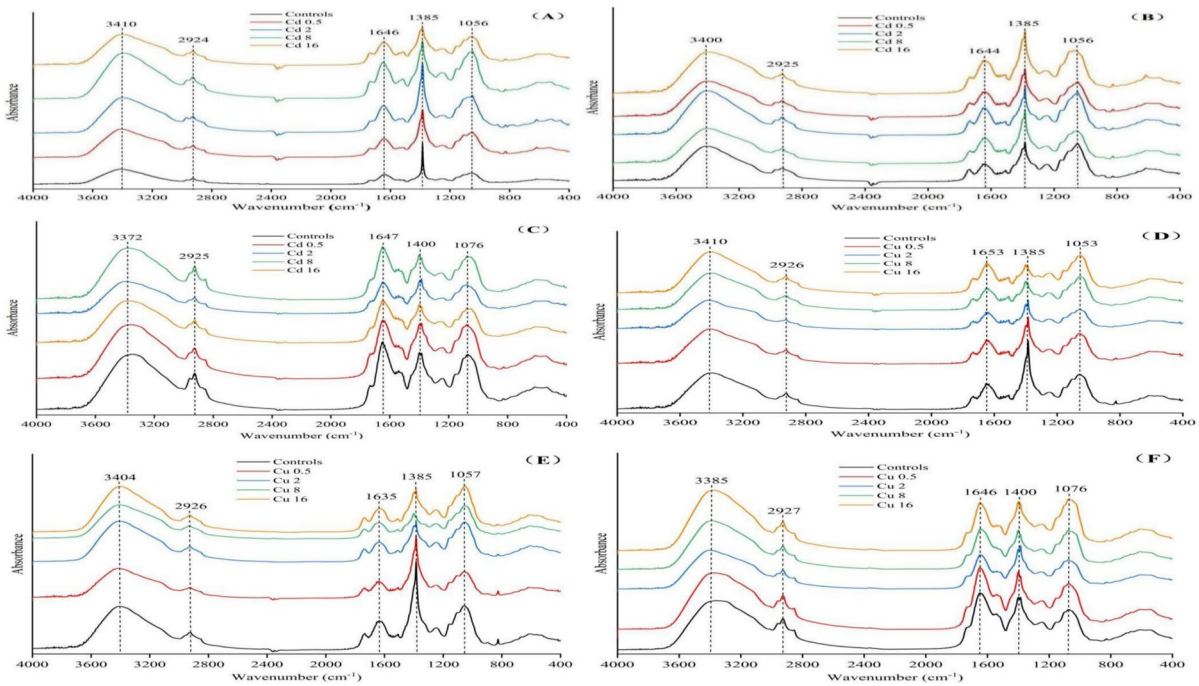

Fig. 1 Fourier transform infrared spectra of *Bidens pilosa* L. roots (**A**), stems (**B**), and leaves (**C**) under Cd treatments, and spectra of roots (**D**), stems (**E**), and leaves (**F**) under Cu treatments

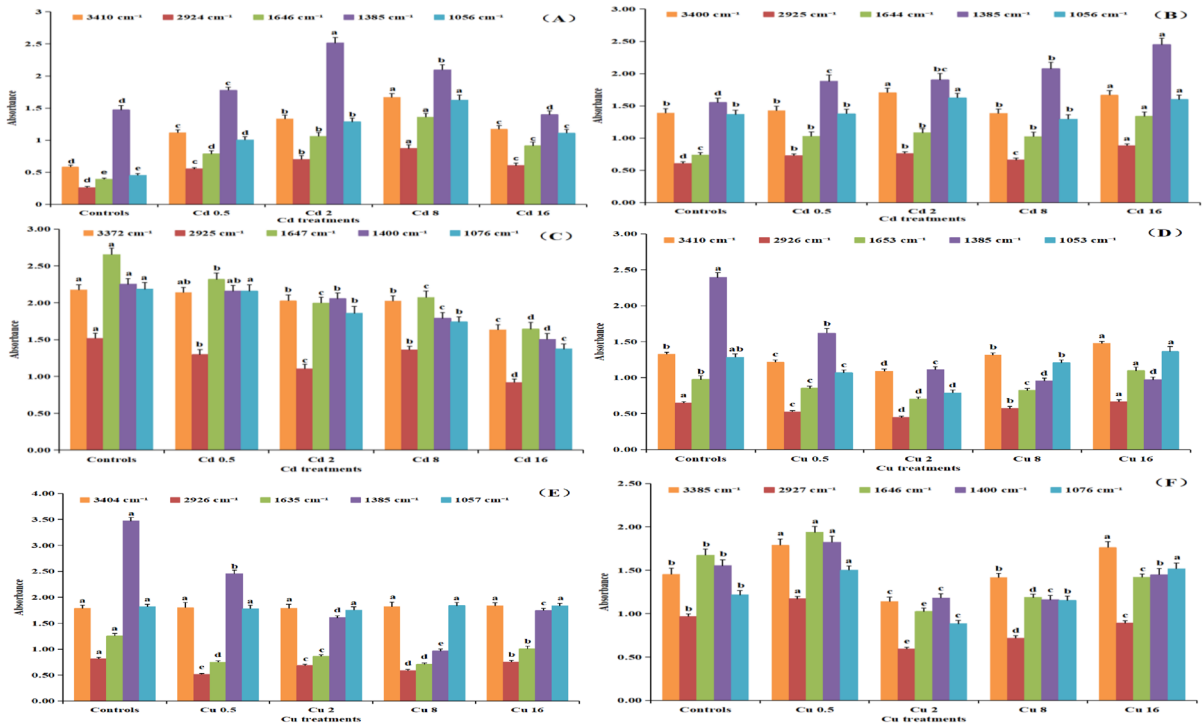

Fig. 2 Comparison of absorbance intensity of characteristic peaks ($1064 \pm 8 cm^{-1}$, 1381 cm^{-1}, 1651 cm^{-1}, 2924 cm^{-1} and 3410 cm^{-1}) in the infrared spectrum of Cd- or Cu-treated *Bidens pilosa* L. seedlings and controls. (Means in different treatments marked with the same lowercase letters are not significantly different at $p < 0.05$)

2925 cm^{-1}, 1644 and 1385 cm^{-1} of the stem spectrum gradually raised with increasing Cd stress concentrations. The maximum occurred at Cd concentration of 16 mg L^{-1}; peak intensities at 3400 and 1056 cm^{-1} under 2 mg L^{-1} Cd stress were also clearly increased compared to other Cd treatments (Fig. 2B). The absorbance intensities of five characteristic peaks in the leaf spectrum decreased significantly in the 16 mg L^{-1} Cd treatments (Fig. 2C).

Absorbance spectra of the roots, stems and leaves of *B. pilosa* were determined and analyzed in response to different Cu levels (Fig. 1D, E, F). The characteristic peaks could be observed by analyzing the infrared spectra (He et al. 2020; Mwamba et al. 2016). The absorbance peaks at 3394 ± 20 cm^{-1} belonged to the stretching vibration of -OH groups, dominant in phenols and alcohols, which were attributed to macromolecular substances, such as cellulose and hemicellulose polysaccharides. The characteristic peaks at 2925 ± 1 cm^{-1} were signals representing $-CH_2$ groups, which could be caused by the presence of membrane lipids and a cell wall containing a large number of lipid compounds. The characteristic peaks at 1645 ± 9 cm^{-1} were acid amides present in the protein conformation. The absorbance peaks at 1390 ± 9 cm^{-1} were attributed to $-CH(CH_3)_2$ groups, and the peaks near 1062 ± 12 cm^{-1} represented C-O stretching vibrations commonly found in long-chain fatty acids, mainly from polyols present in carbohydrates from the cell wall. Compared to controls, the shapes, trends and positions of the peaks in the spectra of *B. pilosa* root, stem and leaf tissues were generally consistent, but several significant differences in peak intensities were still observed between individual Cu treatments. Figure 2D shows that the maximum absorbance intensities of the peaks at 3410 and 1653 cm^{-1} of the root spectrum occurred at Cu concentration of 16 mg L^{-1}. The peak intensities at 1385 cm^{-1} gradually decreased with increasing Cu stress, and there were no significant differences in the peaks at 1053 and 2926 cm^{-1} under 16 mg L^{-1} Cd compared to controls. As shown in Fig. 2E, the intensities of the peaks at 2926, 1635 and 1385 cm^{-1} ($-CH_2$, acid amides, $-CH(CH_3)_2$ groups) of the stem

spectrum decreased significantly compared with controls, and there were no significant variations between the peaks at 3404 and 1057 cm^{-1} compared to controls. Figure 2F indicates that the peak intensities at 2927 and 1646 cm^{-1} of the leaf spectrum were lower in plants subject to Cu stress in the range of 2 ~ 16 mg L^{-1} than in controls, and there were no significant variations between the peaks at 1400 cm^{-1} under 16 mg L^{-1} Cu compared to controls. The maximum intensities of the peaks at 3385 and 1076 cm^{-1} were recorded at Cu concentrations of 0.5 or 16 mg L^{-1}.

In the absorbance spectra of *B. pilosa* root, the peak intensity at 1385 cm^{-1} gradually increased with increasing Cd stress, but decreased under Cu stress. The results indicated that a number of $-CH(CH_3)_2$ groups were produced to combine with Cd in root cell surface. In contrast, the amount of $-CH(CH_3)_2$ groups was reduced with increasing Cu stress. In the same way, the amount of $-CH(CH_3)_2$ groups and protein with acid amides (at 1644 cm^{-1} and 1635 cm^{-1}) were increased in *B. pilosa* cells in the stems of *B. pilosa* in the Cd treatments.

Subcellular distribution and different chemical forms of Cd and Cu in *B. pilosa* seedling

The percentages of Cd/Cu concentrations in different subcellular fractions from root, stem, and leaf tissues of *B. pilosa* seedlings under different treatments were shown from Fig. 3, and the order of Cd proportion in subcellular fractions from roots was: cytoplasm (61.73%) > cell wall (24.93%) > plastid (9.15%) > mitochondria (4.19%) (Fig. 3A). The Cd proportion in cell wall decreased, while in cytoplasm elevated with the increase of Cd stress, and the proportions of Cd in plastid and mitochondria were relatively low. Compared with Cd treatment, the Cu proportions in cell wall of roots were up to 82% under treatments with 8 mg L^{-1} Cu, but Cu proportion in cytoplasm, plastid, mitochondria from roots decreased with the increase of Cu stress. The results indicated that Cd was mainly sequestered in cytoplasm and cell walls of *B. pilosa* roots to cope with Cd stress. By contrast, Cu treatments enhanced Cu accumulation in cell wall of root tissues. As shown from Fig. 3B, the Cd proportions in cell wall were the highest among other subcellular fractions from stems, and Cd proportion in cell wall decreased from 72 to 44% with the increase of Cd stress. Compared with Cd treatment, and the order of Cu proportion in subcellular fractions from shoots was: cell wall (47%) > mitochondria (24%) > plastid (22%) > cytoplasm (6%). The Cu proportion in cell wall raised with the increase of Cu stress, and it was up to 53% under treatments with 8 mg L^{-1} Cu. Results showed that Cd/Cu was mainly concentrated in cell wall of *B. pilosa* stems to cope with stress. From Fig. 3C, the order of Cd proportion in subcellular fractions from leaves was: cell wall (52%) > cytoplasm (26%) > chloroplast (14%) > mitochondria (7%), and the Cd proportion in cell wall decreased with the increase of Cd stress, and it was up to 44% under treatments with 8 mg L^{-1} Cd. Compared with Cd treatment, the Cu proportions in cell wall of leaves were up to 61% under treatments with 8 mg L^{-1} Cu, but Cu proportion in cytoplasm, chloroplast, mitochondria from leaves decreased with the increase of Cu stress. The results indicated that Cd/Cu was mainly concentrated in cell wall of *B. pilosa* leaves to cope with stress.

Different chemical forms of Cd and Cu in roots, stems, and leaves of *B. pilosa* seedlings under different treatments were shown from Fig. 4. The proportion of Cd chemical forms in roots was ordered as follows: Ethanol (68%) > Water (17%) > NaCl (8%) > CH_3COOH (5%) > HCl (1%) > Residue (< 1%) (Fig. 4A). Moreover, the proportion of Cd extracted with ethanol decreased as the Cd stress increased from 0.5 to 8 mg L^{-1}, while the proportion of Cd extracted using water or NaCl increased. By contrast, ethanol extract the highest Cu concentration in all the Cu extracts, and the Cu proportion extracted with ethanol elevated with increasing of Cu stress The results revealed that the proportion of Cd/Cu extracted with ethanol was the highest, and ethanol extracted-Cd/Cu was the main chemical forms in *B. pilosa* seedling roots, easily transferred to the shoots. From Fig. 4B, the proportion of Cd extracted with NaCl (55%) in stems was the highest, follow by extracted with CH_3COOH (21%), Water (15%), HCl (4.3%), Ethanol (3.8%), Residue (0.65%). The proportion of Cd extracted with NaCl went up as the Cd stress increased from 0.5 to 8 mg L^{-1}. Compared with Cd, ethanol extract the highest Cu concentration in all the Cu extracts, and the Cu proportion extracted with ethanol elevated with the increase of Cu stress. But the proportion of Cu extracted with other agents was relatively low. The results showed that the proportion of ethanol-extracted Cd decreased while NaCl-extracted

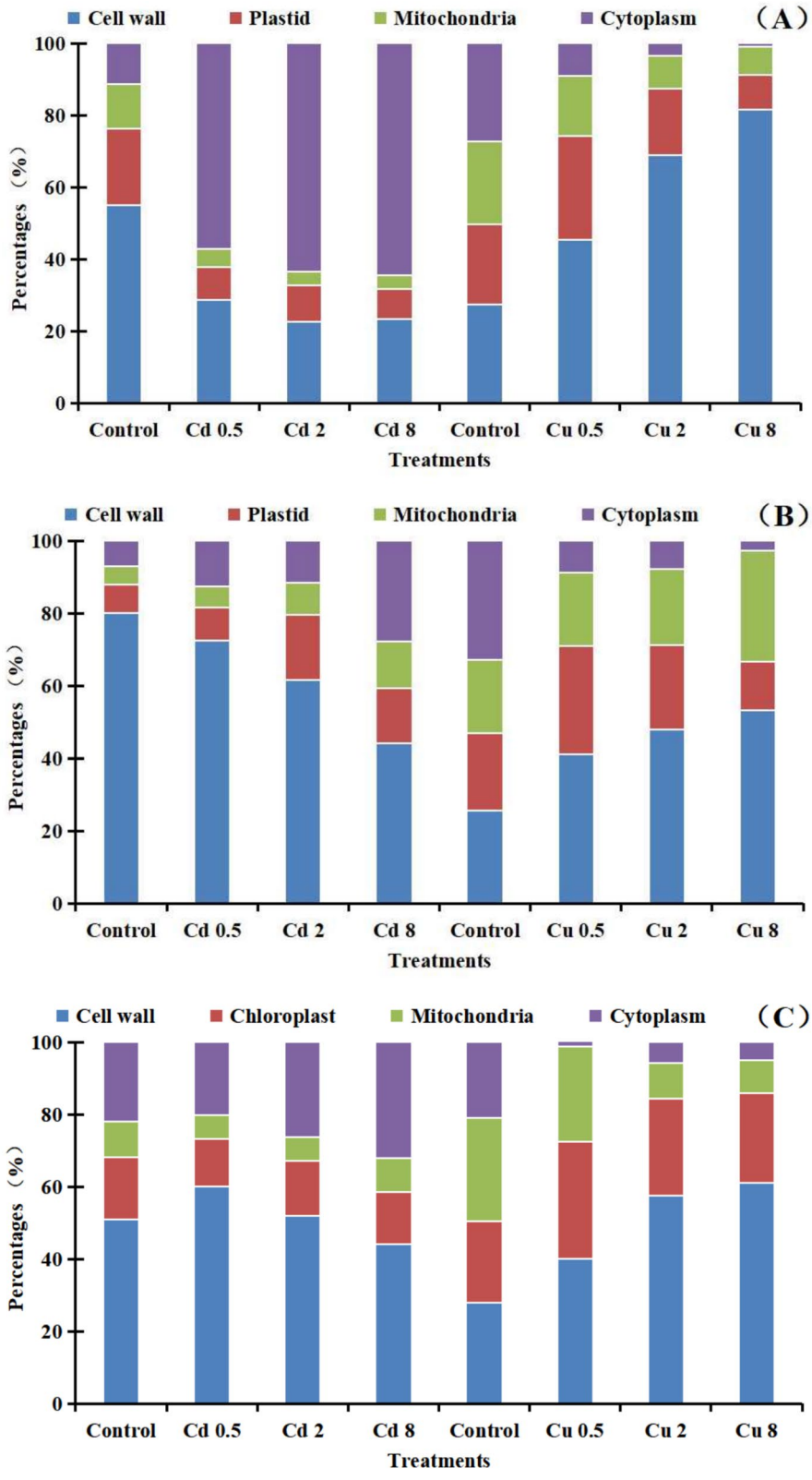

Fig. 3 Percentages of Cd/Cu concentrations in different subcellular fractions from roots (**A**), stems (**B**), and leaf (**C**) of *Bidens pilosa* L. seedlings under different treatments

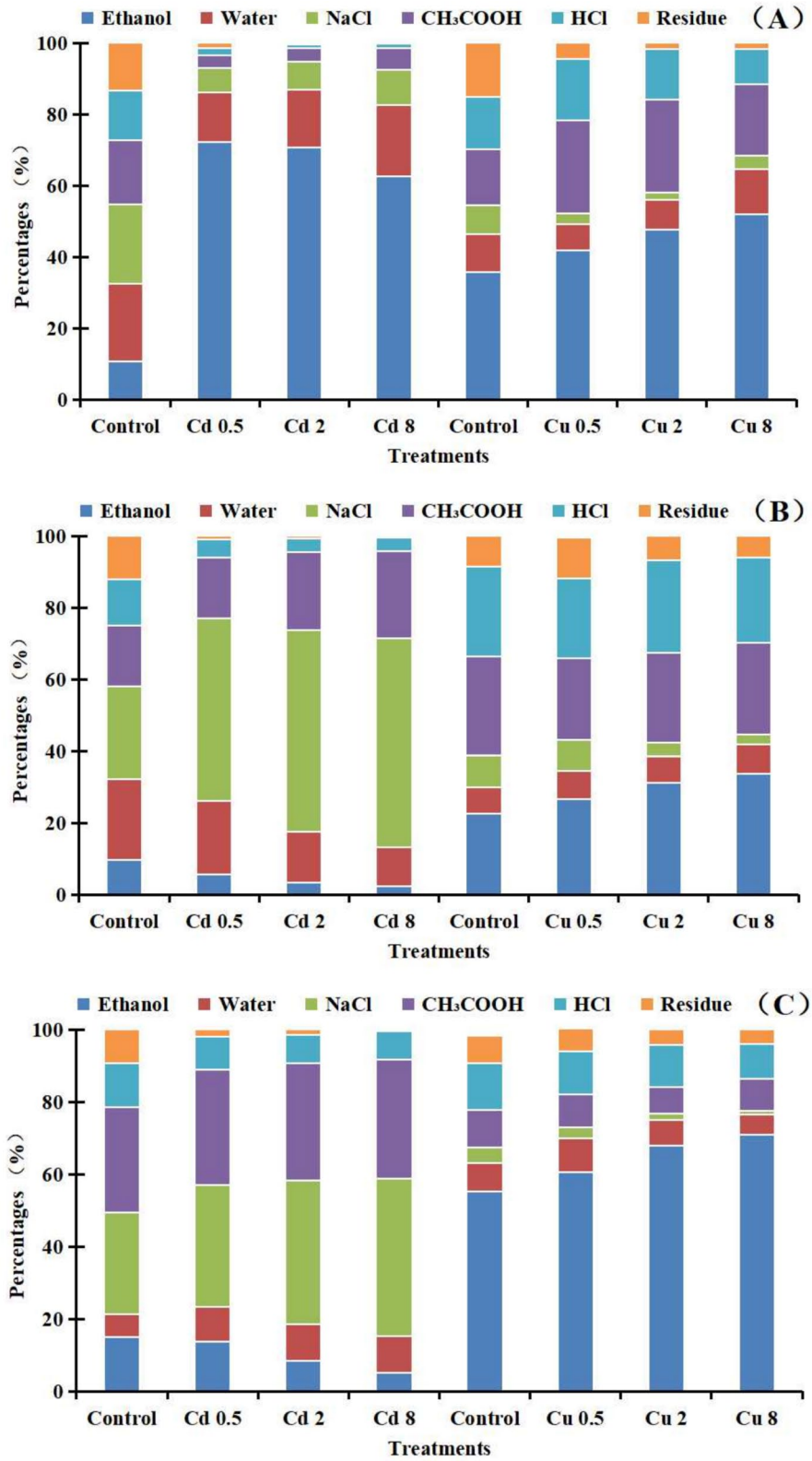

Fig. 4 Different chemical forms of Cd in root (**A**), stem (**B**), and leaf (**C**) of *Bidens pilosa* L. seedlings under different treatments

Cd increased. The transformation of chemical form was the main detoxification mechanism of *B. pilosa* seedling stems coping with Cd stress. But ethanol-extracted Cu remained unchanged in the stems. As shown from Fig. 4C, the proportion of Cd chemical forms in leaves was ordered as follows: NaCl (39%) > CH_3COOH (32%) > Water (9.9%) > Ethanol (9.1%) > HCl (8.2%) > Residue (1.4%), and the proportion of Cd extracted with NaCl or CH_3COOH elevated with Cd stress increased from 0.5 to 8 mg L^{-1}. By contrast, ethanol extract the highest Cu concentration in all the Cu extracts, and the proportion of Cu extracted with other agents was relatively low. The results indicated that the detoxification mechanism of *B. pilosa* leaves was by means of elevating the proportion of NaCl-extracted Cd and lowering the ethanol-extracted Cd. But the leaves had no detoxification ability to Cu.

Discussion

Dai et al. (2017) found that the Cd concentration in *B. pilosa* shoots was 405.91 mg kg^{-1} after four weeks of growth in soils with Cd concentration at 64 mg/kg, and the translocation and enrichment factors were 1.14 and 6.33, respectively. Cd concentration in shoots was 1652 mg kg^{-1}, when the plants were cultivated in nutrient solutions with a Cd concentration of 64 mg/kg, and the translocation and enrichment factors were 1.49 and 25.81, respectively. The shoot Cd concentrations in *B. pilosa* in this study were less than those reported by Dai et al. (2017). This may be due to phosphate co-precipitation forming in the root apoplast. Liu et al. (2019) identified *Lantana camara* L. as a Cd hyperaccumulator using dose gradient experiments and field tests. These authors reported that the seedlings were grown in the contaminated soils with Cd level lower than 100 mg kg^{-1}, and the plants showed high Cd tolerance, without obvious damage and reduction in shoot biomass compared to controls. Importantly, the bioaccumulation and translocation factors were all > 1, and the Cd concentration in the shoots was also higher than 100 mg kg^{-1} in all treatments. Xv et al. (2020) found that Cu enrichment in *Sedum alfredii* mainly occurred in the roots, with only a minimal amount of Cu translocation to the stem. The high tolerance of *S. alfredii* to Cu resulted from homeostasis in root cells, and vascular tissues were the dominant location of Cu restriction. Our research suggested that *B. pilosa* exhibited some basic characteristics of Cd hyperaccumulator in hydroponic culture and shoot Cd concentration was up to 100 mg kg^{-1} in the 0.5 mg L^{-1} Cd treatment. The TF of *B. pilosa* was 1.26, and the roots showed high tolerance to Cd, the results here might be different to other researchers, which were originated from a different ecotype of *B. pilosa* or under different growth conditions. However, this species did not show Cu hyperaccumulator or accumulator properties, because the TFs were all < 1 in Cu treatments. In addition, most Cu concentrated in the roots, and root biomass decreased under Cu stress conditions.

Plants produce metal-binding proteins such metallothioneins and phytochelatins that chelate and sequester heavy metals (REF). These proteins bind to metals and prevent them from interfering with important physiological processes thereby reducing their toxicity (Fahad et al. 2024, 2021). Mwamba et al. (2016) found that the main chemical forms of Cd integration in rapeseed (*Brassica napus*) roots were pectates and proteins and phosphate-bound Cu was the dominant fraction in the cell walls. Bora and Sarma (2021) analyzed the FTIR spectrum of *Ceratopteris pteridoides* root samples and observed strong and broad peaks in the mid-infrared region of 3500 ~ 3200 cm^{-1}, 1700 ~ 1600 cm^{-1}, 1500 ~ 1400 cm^{-1}, 1300 ~ 1200 cm^{-1} and 800 ~ 400 cm^{-1}. These peaks represented N–H or O–H, N–H, C-H, P = O or C-O or C-O-P, C-O–H or C-S functional groups, which played significant roles in Cd binding and corresponded to lignin, cellulose, proteins, lipids, phospholipids or nucleic acids, disulfide bonds and other metabolites. The latter authors also found that the mechanism of Cd tolerance in *Ceratopteris pteridoides* roots was based on the accumulation of electron-dense material on the cell walls. Wu et al. (2020) used FTIR analysis to investigate the mechanisms of Cd resistance in rapeseed (*Brassica napus*) shoots with the addition of boron (B) and suggested that the increase in pectin, protein, carbohydrate and cellulose contents in the cell walls alleviated Cd toxicity. Su et al. (2017) found that amide, hydroxyl, carbonyl and thiol functional groups were involved in Cd accumulation and uptake in duckweed (*Spirodela polyrhiza*) roots on the basis of FTIR spectrometry analysis, and reported that Cd stress could induce the accumulation

of soluble sugars. Dumont et al. (2022) studied the toxic effects of nano-CuO on *Myriophyllum spicatum* seedlings and suggested that the composition and structure of biomacromolecules (such as proteins, carbohydrates, phenols and cellulosic compounds) in the plant samples markedly changed under different nano-CuO treatments (from 5 to 70 mg L^{-1}). Rana et al. (2018) argued that the characteristic peaks at 1385 ~ 1394 cm^{-1}represented stretching vibrations of oxygen and hydrogen, indicating changes in cellulose contents in orchardgrass (*Dactylis glomerata* L.) leaf tissue; on the other hand, the absorbance peaks at 1373 ~ 1375 cm^{-1} were shown to represent suberin-like aliphatic compounds in kentucky bluegrass (*Poa pratensis* L.) leaves. Sawalha et al. (2007) used FTIR to investigate the identity of functional groups involved in Cd binding in different tissues of saltbush (*Atriplex canescens*) shoots after acidic methanol modification and found that the carboxyl group was the dominant one in Cd binding sites. Zhang et al. (2021) found that the detoxification mechanisms of annual fleabane (*Erigeron annuus*) in response to 200 μmol L^{-1} Cd stress involved the secretion of dissolved organic matter (DOM) by roots, and DOM mainly consisted of several functional groups, such as aromatic structures, tannins and carbohydrates, which played important roles in stress management. Yu et al. (2020) analyzed the FTIR spectral information of root, stem and leaf samples from *Conyza canadensis* (L.) Cronq., and found that the shapes of characteristic peaks remained unchanged in Cd treatments and controls, but the absorbance intensity of the roots was stronger under high Cd concentration conditions, indicating that large quantities of proteins and amino acids were produced as nitrogen sources to manage Cd toxicity and sustain intracellular environments. Lan et al. (2019) investigated Cd distribution and accumulation in the roots, stems and leaves of the hyperaccumulator *Microsorum pteropus* and found that Cd was mainly sequestrated and stored in the roots and leaf cell wall fraction; in addition to the cell wall, Cd was also found in the stem cytoplasm fraction. He et al. (2020) analyzed subcellular fractions of different tissues from castor (*Ricinus communis*) seedlings using FTIR and discovered that functional groups (carboxyl, hydroxyl, amide and amino groups) provided a large number of sites for Cd binding on the cell wall. Our research also suggested that typical functional groups (e.g., -OH; $-CH_2$ and $-CH(CH_3)_2$) and corresponding biochemical regions, such as acid amides and lipids were involved in the co-precipitation and complexation of *B. pilosa* root cells as a response to Cd stress.

Pan et al. (2019) discovered that manganese (Mn) was isolated in cell wall and vacuole of pink plume-poppy (*Macleaya cordata*). In addition, most Mn was sequestered in low-toxicity compound such as oxalates, pectates, phosphates and protein. Teng et al. (2021) suggested that the vacuoles of *S. nigrum* leaf cells were main locations for Cd storage, and the proportion of vacuolar Cd in protoplasts was up to 83.37% under 50 μM Cd treatments. In addition, the chelation state Cd was the dominated chemical form in protoplast. Luo et al. (2024) demonstrated that More than 50% of Cd was trapped in cell walls from leaves of reed fescue (*Festuca arundinacea*). The cell wall binding Cd was a key pathway for detoxification. The cell wall served as a protective barrier against Cd penetration into plant cells. Some plants changed the makeup of their cell walls, increased the binding of Cd to pectins, hemicelluloses, and other structural elements (Ahmad et al. 2022; Irfan et al. 2021; Fahad et al. 2020). Cd-induced changed in cell wall composition, increased lignification and changed in polysaccharide content, contributed to a physical barrier that restricted the entry of Cd ions into plant cells (Song et al. 2024). An et al. (2023) verified that Cd was mainly accumulated in *Platycodon grandiflorum* roots, and was predominantly sequestered in cell wall. The chemical state of Cd was characterized by low mobility and toxicity, and the proportion of Cd in cytoplasm increased under Cd stress. The accumulation and detoxification mechanism of Cd by *P. grandiflorum* were root retention, cell wall deposition, vacuole isolation, low mobility and toxicity transformation. Wu et al. (2016) showed that Cd proportion in cell wall of *S. matsudana* roots was 53% under 10 μM Cd stress, and concluded that cell wall of roots might serve as the first barrier to bind and reduce free Cd ions entering the cytoplasm. The proportion of ethanol-extracted and water-extracted Cd were relatively low, and the proportion of NaCl-extracted Cd was 42% with 10 μM Cd treatment. Xin et al. (2014) compared the difference of Cd uptake and translocation between low and high accumulation cultivars of hot pepper by measuring the subcellular distributions and chemical forms of Cd, and concluded that the cytoplasm stored the majority of Cd in the roots of

both varieties, and a minimal amount of Cd existed in organelle fraction. These researches were basically consistent with our results. Our results showed that most of Cd was mainly concentrated in cytoplasm of *B. pilosa* roots, and sequestered in cell wall of stems and leaves to cope with stress. The detoxification mechanism of *B. pilosa* was to elevate the proportion of NaCl-extracted Cd and lower ethanol-extracted Cd.

Conclusions

Our work showed that the key compounds associated with Cd hyperaccumulation in *B. pilosa* were alcohols, phenols, acid amides and lipids by using FTIR, focusing specifically on differences in functional group characteristics. The study further confirmed that *B. pilosa* was a Cd hyperaccumulator, but not a Cu hyperaccumulator. The FTIR results indicated that the characteristic peaks corresponded to the following functional groups and biochemical regions: phenolic and alcohol -OH groups, $-CH_2$ groups, acid amides, $-CH(CH_3)_2$ groups and fatty acids. The amount of these functional groups increased with increasing Cd stress concentrations, and corresponding macromolecules in cells in the stems/roots of *B. pilosa* participated in response to Cd stress stimuli. Especially, the absorbance peak intensity at 1385 cm^{-1} in root spectra increased gradually with increasing Cd stress, but decreased under Cu stress. The results indicated that a number of $-CH(CH_3)_2$ groups were produced to combine with Cd in root cell surface. In contrast, the amount of $-CH(CH_3)_2$ groups was reduced with increasing Cu stress, the amount of $-CH(CH_3)_2$ groups and protein with acid amides were raising in cells in the stems of *B. pilosa* under Cd treatments. Results also revealed that most of Cd was mainly sequestered in cytoplasm and cell walls of *B. pilosa* roots to cope with Cd stress. Cu was only trapped in cell walls of root tissues, and majority of Cd/Cu was sequestered in cell walls of *B. pilosa* stems and leaves to cope with stress. The detoxification of *B. pilosa* was completed by means of elevating the proportion of NaCl-extracted Cd and lowering ethanol-extracted Cd. But there were no significant changes for the proportion of ethanol-extracted Cu. The hyperaccumulating and detoxification mechanisms of *B. pilosa* might be regulation of the corresponding macromolecules (such as alcohols and phenols, proteins and lipids, etc.) in cells, Cd immobilization and compartmentalization in cytoplasm and cell walls, and transformation of Cd chemical forms. The response to Cd stress of *B. pilosa* represented a complex physiological and biochemical metabolic process. So the research of Cd subcellular distributions and chemical forms should be combined with various omics level methods such as genomics, transcriptomics, proteomics and metabolomics to study the relationships between genes, proteins and metabolites to improve the understanding of *B. pilosa* responses to Cd stress.

Author contribution Siqi Wang: Data processing, Writing – original draft & detection. Jiayi Bai: Resources, cultivation & detection. Huiping Dai: Data curation, Formal analysis, Writing – review & editing. Jie Zhan: Validation, Writing – review & editing. Liping Ren: Detection & data processing. Brett H. Robinson: Validation, Writing – review & editing. Chengzhi Jiang: Detection & data processing. Shuang Cui: Detection & data processing. Lidia Skuza: Validation, Writing – review & editing. Shuhe Wei: Conceptualization, Methodology, Project administration, Supervision.

Funding This work was supported by Sanqin Talents, Shaanxi Provincial First-class Team– " Contaminated Soil Remediation and Resource Utilization Innovation Team at Shaanxi University of Technology", the National Natural Science Foundation of China (32471703), Shaanxi University of Technology Research Ability Enhancement Project (SLGNL202405), Qin Chuangyuan "Scientists+Engineers" Team Construction in Shaanxi Province (2024QCY-KXJ-104), the project of Foreign Experts Bureau of China (S20240182, 2025WZ-YBXM-19, 2025WZ-YBXM-29), Shaanxi Province City-University Co-Construction Project (SXZJ-2301), Qinba Bioremediation and Resource Development Research Innovation and Introduction Base (2025YZ-YIPT-41; S2022-ZC-GXYZ-0029), the program financed by Poland Minister of Science under the "Regional Excellence Initiative" for 2024–2027, the General Program of the National Natural Science Foundation of China (41671324), the General Program from the Education Department of Liaoning Province (LJKMZ20220595). Basic scientific research project of Liaoning Provincial Department of Education (General Project) (JYTMS20230179).

Data availability Data will be made available on request.

Declarations

Competing interest The authors declare that they have no known competing financial interests or personal relationships that could have appeared to influence the work reported in this paper.

References

Ahmad W, Khan A, Zeeshan M, Ahmad I, Adnan M, Fahad S, Solaiman Z (2022) Relative efficiency of biochar particles of different sizes for immobilising heavy metals and improving soil properties. Crop Pasture Sci 74:112–120

An J, Wang X, Jing Y, Huang J, Wang Q, Zhang G, Gao J, Peng L, Huang W, Yan Y (2023) Subcellular distribution and chemical forms of cadmium in the medicine food homology plant *Platycodon grandiflorum* (Jacq.) A.DC. Phyton (0031-9457) 92(5):1405–1420

Bora MS, Sarma KP (2021) Anatomical and ultrastructural alterations in *Ceratopteris pteridoides* under cadmium stress: A mechanism of cadmium tolerance. Ecotoxicol Environ Saf 218:112285

Cai FJ, Wang L, Zhao W, Tian JL, Kong DG, Liu Q, Sun XH, Zhou HL (2022) Phytochemical and chemotaxonomic investigations on the whole herbs of *Bidens procera* L.C.Xu ex X.W.Zheng. Biochem Syst Ecol 101:104395

Chow YY, Ting ASY (2019) Influence of fungal infection on plant tissues: FTIR detects compositional changes to plant cell walls. Fungal Ecol 37:38–47

Dai H, Wei S, Twardowska I, Han R, Xu L (2017) Hyperaccumulating potential of *Bidens pilosa* L. for Cd and elucidation of its translocation behavior based on cell membrane permeability. Environ Sci Pollut Res 24(29):23161–23167

Dumont ER, Elger A, Azéma C, Michel HC, Surble S, Larue C (2022) Cutting-edge spectroscopy techniques highlight toxicity mechanisms of copper oxide nanoparticles in the aquatic plant *Myriophyllum spicatum*. Sci Total Environ 803:150001

Fahad S, Hasanuzzaman M, Alam M, Ullah H, Saeed M, Khan IA, Adnan M (eds) (2020) Environment, climate, plant and vegetation growth. Springer International Publishing, Berlin/Heidelberg, Germany, pp 397–419

Fahad S, Saud S, Yajun C, Chao W, Depeng W (Eds.) (2021) Abiotic stress in plants. Intech Open United Kingdom 2021.

Fahad S, Saud S, Nawaz T, Gu L, Ahmad M, Zhou R (Eds.) (2024) Environment, Climate, Plant and Vegetation Growth (2nd edition). Springer Nature Switzerland AG 2024.

Feng Y, Wang Q, Meng Q, Liu Y, Pan F, Luo S, Wu Y, Ma L, Yang X (2019) Chromosome doubling of *Sedum alfredii* Hance: A novel approach for improving phytoremediation efficiency. J Environ Sci 86:87–96

Hamid Y, Tang L, Yaseen M, Hussain B, Zehra A, Aziz MZ, He Z, Yang X (2019) Comparative efficacy of organic and inorganic amendments for cadmium and lead immobilization in contaminated soil under rice-wheat cropping system. Chemosphere 214:259–268

He C, Zhao Y, Wang F, Oh K, Zhao Z, Wu C, Zhang X, Chen X, Liu X (2020) Phytoremediation of soil heavy metals (Cd and Zn) by castor seedlings: Tolerance, accumulation and subcellular distribution. Chemosphere 252:126471

Heredia B, Tapia R, Young BJ, Hasuoka P, Pacheco P, Roqueiro G (2022) Phytoextraction of Cu, Cd, Zn and As in four shrubs and trees growing on soil contaminated with mining waste. Chemosphere 308:136146

Irfan M, Mudassir M, Khan MJ, Dawar KM, Muhammad D, Mian IA, Ali W, Fahad S, Saud S, Hayat Z, Nawaz T, Khan SA, Alam S, Ali B, Banout J, Ahmed S, Mubeen S, Danish S, Datta R, Elgorban AM, Dewil R (2021) Heavy metals immobilization and improvement in maize (*Zea mays* L.) growth amended with biochar and compost. Sci Rep 11(1):18416

Lan XY, Yan YY, Yang B, Li XY, Xu FL (2019) Subcellular distribution of cadmium in a novel potential aquatic hyperaccumulator-*Microsorum pteropus*. Environ Pollut 248:1020–1027

Li Z, Yang Y, Guan W, Yu H, Zou L, Cui J, Teng Y (2023) Insight into the subcellular mechanism of maximizing Cd accumulation in hyperaccumulator *Solanum nigrum* L. under the action of biodegradable chelating agent. Environ Exp Bot 207:105226

Liu S, Ali S, Yang R, Tao J, Ren B (2019) A newly discovered Cd-hyperaccumulator *Lantana camara* L. J Hazard Mater 371:233–242

Liu X, Renard CM, Bureau S, Le Bourvellec C (2021) Revisiting the contribution of ATR-FTIR spectroscopy to characterize plant cell wall polysaccharides. Carbohyd Polym 262:117935

Luo J, Feng S, Li M, He Y, Deng Y, Cao M (2024) Effect of magnetized water irrigation on Cd subcellular allocation and chemical forms in leaves of *Festuca arundinacea* during phytoremediation. Ecotoxicol Environ Saf 277(116376):455–462

Mwamba TM, Li L, Gill RA, Islam F, Nawaz A, Ali B, Farooq MA, Lwalaba JL, Zhou WJ (2016) Differential subcellular distribution and chemical forms of cadmium and copper in *Brassica napus*. Ecotoxicol Environ Saf 134:239–249

Omara T, Kagoya S, Openy A, Omute T, Ssebulime S, Kiplagat KM, Bongomin O (2020) Antivenin plants used for treatment of snakebites in Uganda: ethnobotanical reports and pharmacological evidences. Trop Med Health 48(1):1–16

Pan F, Meng Q, Wang Q, Luo S, Chen B, Khan KY, Yang X, Feng Y (2016) Endophytic bacterium *Sphingomonas* SaMR12 promotes cadmium accumulation by increasing glutathione biosynthesis in *Sedum alfredii* Hance. Chemosphere 154:358–366

Pan G, Zhang H, Liu W, Liu P (2019) Integrative study of subcellular distribution, chemical forms, and physiological responses for understanding manganese tolerance in the herb *Macleaya cordata* (papaveraceae). Ecotoxicol Environ Saf 181:455–462

Pasricha S, Mathur V, Garg A, Lenka S, Verma K, Agarwal S (2021) Molecular mechanisms underlying heavy metal uptake, translocation and tolerance in hyperaccumulators-an analysis: Heavy metal tolerance in hyperaccumulators. Environ Challenges 4:100197

Rana R, Herz K, Bruelheide H, Dietz S, Haider S, Jandt U, Pena R (2018) Leaf Attenuated Total Reflection Fourier Transform Infrared (ATR-FTIR) biochemical profile of grassland plant species related to land-use intensity. Ecol Indic 84:803–810

Sawalha MF, Peralta-Videa JR, Saupe GB, Dokken KM, Gardea-Torresdey JL (2007) Using FTIR to corroborate the identity of functional groups involved in the binding of Cd and Cr to saltbush (*Atriplex canescens*) biomass. Chemosphere 66(8):1424–1430

Sharma S, Uttam KN (2017) Rapid analyses of stress of copper oxide nanoparticles on wheat plants at an early stage by laser induced fluorescence and attenuated total reflectance Fourier transform infrared spectroscopy. Vib Spectrosc 92:135–150

Sharma S, Uttam KN (2019) Non-destructive and rapid interrogation of biochemical response of the leaves of wheat seedlings towards Al_2O_3 nanoparticles stress using attenuated total reflectance Fourier transform infrared spectroscopy. Vib Spectrosc 100:142–151

Song J, Sun Z, Saud S, Fahad S, Nawaz T (2024) Exploring the deleterious effects of heavy metal cadmium on antioxidant defense and photosynthetic pathways in higher plants. Plant Stress 100716

Su C, Jiang Y, Li F, Yang Y, Lu Q, Zhang T, Hu D, Xu Q (2017) Investigation of subcellular distribution, physiological, and biochemical changes in *Spirodela polyrhiza* as a function of cadmium exposure. Environ Exp Bot 142:24–33

Sun Y, Zhou Q, Wang L, Liu W (2009) Cadmium tolerance and accumulation characteristics of *Bidens pilosa* L. as a potential Cd-hyperaccumulator. J Hazard Mater 161(2–3):808–814

Suresh S, Karthikeyan S, Jayamoorthy K (2016) FTIR and multivariate analysis to study the effect of bulk and nano copper oxide on peanut plant leaves. J Sci-Adv Mater Dev 1(3):343–350

Teng Y, Yu A, Tang YM, Jiang ZY, Guan WJ, Li ZS, Yu HY, Zou LY (2021) Visualization and quantification of cadmium accumulation, chelation and antioxidation during the process of vacuolar compartmentalization in the hyperaccumulator plant *Solanum nigrum* L. Plant Sci 310:110961

Tolmacheva AA, Rogozhin EA, Deryabin DG (2014) Antibacterial and quorum sensing regulatory activities of some traditional Eastern-European medicinal plants. Acta Pharmaceut 64(2):173–186

Wang S, Dai H, Skuza L, Chen Y, Wei S (2022) Difference in Cd^{2+} flux around the root tips of different soybean (*Glycine max* L.) cultivars and physiological response under mild cadmium stress. Chemosphere 297:134120

Wei S, Zhou Q (2008) Screen of Chinese weed species for cadmium tolerance and accumulation characteristics. Int J Phytoremediat 10(6):584–597

Wei S, Zhou Q, Zhan J, Wu Z, Sun T, Lyubu Y, Prasad MNV (2010) Poultry manured *Bidens tripartite* L. extracting Cd from soil-potential for phytoremediating Cd contaminated soil. Bioresource Technol 101(22):8907–8910

Wei H, Huang M, Quan G, Zhang J, Liu Z, Ma R (2018) Turn bane into a boon: Application of invasive plant species to remedy soil cadmium contamination. Chemosphere 210:1013–1020

Wu H, Wang J, Li B, Ou Y, Wang J, Shi Q, Jiang W, Liu D, Zou J (2016) *Salix matsudana* koidz tolerance mechanisms to cadmium: Uptake and accumulation, subcellular distribution, and chemical forms. Pol J Environ Stud 25(4):1739–1747

Wu X, Song H, Guan C, Zhang Z (2020) Boron mitigates cadmium toxicity to rapeseed (*Brassica napus*) shoots by relieving oxidative stress and enhancing cadmium chelation onto cell walls. Environ Pollut 263:114546

Xin J, Huang B, Dai H, Liu A, Zhou W, Liao K (2014) Characterization of cadmium uptake, translocation, and distribution in young seedlings of two hot pepper cultivars that differ in fruit cadmium concentration. Environ Sci Pollut Res 21:7449–7456

Xu M, Lin Y, da Silva EB, Cui Q, Gao P, Wu J, Ma LQ (2022) Effects of copper and arsenic on their uptake and distribution in As-hyperaccumulator *Pteris vittata*. Environ Pollut 300:118982

Xv L, Ge J, Tian S, Wang H, Yu H, Zhao J, Lu L (2020) A Cd/Zn Co-hyperaccumulator and Pb accumulator, *Sedum alfredii*, is of high Cu tolerance. Environ Pollut 263:114401

Yang Q, Shohag MJI, Feng Y, He Z, Yang X (2017) Transcriptome comparison reveals the adaptive evolution of two contrasting ecotypes of Zn/Cd hyperaccumulator *Sedum alfredii* hance. Front Plant Sci 8:425

Yu S, Sheng L, Zhang C, Deng H (2018) Physiological response of *Arundo donax* to cadmium stress by Fourier transform infrared spectroscopy. Spectrochim Acta A 198:88–91

Yu S, Sheng L, Mao H, Huang X, Luo L, Li Y (2020) Physiological response of *Conyza canadensis* to cadmium stress monitored by Fourier transform infrared spectroscopy and cadmium accumulation. Spectrochim Acta A 229:118007

Yu H, Yang A, Wang K, Li Q, Ye D, Huang H, Zhang X, Wang Y, Zheng Z, Li T (2021) The role of polysaccharides functional groups in cadmium binding in root cell wall of a cadmium-safe rice line. Ecotoxicol Environ Saf 226:112818

Yu F, Tang S, Shi X, Liang X, Liu K, Huang Y, Li Y (2022) Phytoextraction of metal (loid) s from contaminated soils by six plant species: A field study. Sci Total Environ 804:150282

Yu SH, Deng HP, Zhang B, Liu ZX, Lin JJ, Sheng L, Qi JS (2022) Physiological response of *Vetiveria Zizanioides* to cadmium stress revealed by Fourier transform infrared spectroscopy. Spectrosc Lett 55(3):157–165

Zeng HY, Chen LH, Yang Y, Deng X, Zhou XH, Zeng QR (2019) Basal and foliar treatment using an organic fertilizer amendment lowers cadmium availability in soil and cadmium uptake by rice on field micro-plot experiment planted in contaminated acidic paddy soil. Soil Sediment Contam 28(1):1–14

Zhang H, Heal K, Zhu X, Tigabu M, Xue Y, Zhou C (2021) Tolerance and detoxification mechanisms to cadmium stress by hyperaccumulator *Erigeron annuus* include molecule synthesis in root exudate. Ecotoxicol Environ Saf 219:112359

Zou J, Wang Y, Wang S, Shang X (2023) Ca alleviated Cd-induced toxicity in *Salix matsudana* by affecting Cd absorption, translocation, subcellular distribution, and chemical forms. J Plant Physiol 281:153926